

## References and Notes

- (1) D. J. Massa, J. L. Schrag, and J. D. Ferry, *Macromolecules*, **4**, 210 (1971).
- (2) K. Osaki and J. L. Schrag, *Polym. J.*, **2**, 541 (1971).
- (3) J. W. M. Noordermeer, O. Kramer, F. H. M. Nestler, J. L. Schrag, and J. D. Ferry, *Macromolecules*, **8**, 539 (1975).
- (4) J. W. M. Noordermeer, J. D. Ferry, and N. Nemoto, *Macromolecules*, **8**, 672 (1975).
- (5) D. J. Massa and J. L. Schrag, *J. Polym. Sci., Part A-2*, **10**, 71 (1972).
- (6) P. E. Rouse, *J. Chem. Phys.*, **21**, 1272 (1953).
- (7) B. H. Zimm, *J. Chem. Phys.*, **24**, 269 (1956).
- (8) J. D. Ferry, "Viscoelastic Properties of Polymers", 2nd ed, Wiley, New York, N.Y., 1970.
- (9) R. S. Moore, H. J. McSkimin, C. Gieniewski, and P. Andreach, Jr., *J. Chem. Phys.*, **47**, 3 (1967); **50**, 5088 (1969).
- (10) G. B. Thurston and A. Peterlin, *J. Chem. Phys.*, **46**, 4881 (1967).
- (11) A. Peterlin, *J. Polym. Sci., Part A-2*, **5**, 179 (1967).
- (12) G. B. Thurston and J. L. Schrag, *J. Polym. Sci., Part A-2*, **6**, 1331 (1968).
- (13) A. Peterlin, *J. Polym. Sci., Part B*, **10**, 101 (1972).
- (14) B. J. Cooke and A. J. Matheson, *J. Chem. Soc., Faraday Trans. 2*, **72**, 679 (1976).
- (15) J. W. Miller and J. L. Schrag, *Macromolecules*, **8**, 361 (1975).
- (16) J. T. Fong and A. Peterlin, *J. Res. Natl. Bur. Stand., Sect. B*, **80**, 273 (1976).
- (17) M. Fixman and J. Kovac, *J. Chem. Phys.*, **61**, 4939, 4950 (1974); **63**, 935 (1975).
- (18) M. Fixman and G. T. Evans, *J. Chem. Phys.*, **64**, 3474 (1976).
- (19) M. Doi, H. Nakajima, and Y. Wada, *Colloid Polym. Sci.*, **253**, 905 (1975); **254**, 559 (1976).
- (20) S. F. Edwards and K. F. Freed, *J. Chem. Phys.*, **61**, 1189 (1974).
- (21) S. A. Adelman and K. F. Freed, *J. Chem. Phys.*, in press.
- (22) P. G. de Gennes, *J. Chem. Phys.*, **66**, 5825 (1977).
- (23) R. Cerf, *Chem. Phys. Lett.*, **24**, 317 (1974).
- (24) A. S. Lodge and Yeen-Jing Wu, MRC Technical Summary Report No. 1250, Mathematics Research Center, University of Wisconsin-Madison, Madison, Wis. 1972.
- (25) K. Osaki and J. L. Schrag, *J. Polym. Sci., Polym. Phys. Ed.*, **11**, 549 (1973).
- (26) K. Osaki, Y. Mitsuda, J. L. Schrag, and J. D. Ferry, *Trans. Soc. Rheol.*, **18**, 395 (1974).
- (27) J. W. Miller, B. G. Brueggeman, T. P. Lodge, M. G. Minnick, and J. L. Schrag, *Macromolecules*, to be submitted.
- (28) J. Lamb and A. J. Matheson, *Proc. R. Soc. London, Ser. A*, **281**, 207 (1964).
- (29) R. M. Johnson, J. L. Schrag, and J. D. Ferry, *Polym. J.*, **1**, 742 (1970).
- (30) A. Peterlin, private communication.
- (31) M. Fixman and G. T. Evans, private communication.
- (32) F. C. Wang and B. H. Zimm, *J. Polym. Sci., Polym. Phys. Ed.*, **12**, 1619, 1638 (1974).
- (33) M. Kurata and W. H. Stockmayer, *Fortschr. Hochpolym.-Forsch.*, **3**, 196 (1963).
- (34) J. D. Ferry, private communication.
- (35) K. Osaki, J. L. Schrag, and J. D. Ferry, *Macromolecules*, **5**, 144 (1972).
- (36) H. Nomura and Y. Miyahara, *Polym. J.*, **8**, 30 (1976).
- (37) W. H. Stockmayer and K. Matsuo, *Macromolecules*, **5**, 766 (1972).
- (38) K. Ono, H. Shintani, O. Yano, and Y. Wada, *Polym. J.*, **5**, 164 (1973).

## Spin Relaxation and Local Motion in Solutions of Poly(2,6-dimethyl-1,4-phenylene oxide)

Alan Anthony Jones\* and Ronald P. Lubianez

*Jeppson Laboratory, Department of Chemistry, Clark University, Worcester, Massachusetts 01610. Received May 18, 1977*

**ABSTRACT:** The spin-lattice relaxation time of the methyl protons of poly(2,6-dimethyl-1,4-phenylene oxide) dissolved in  $\text{CDCl}_3$  was measured as a function of molecular weight, temperature, and concentration. At a given temperature and concentration, the molecular weight dependence of the spin-lattice relaxation times was interpreted in terms of correlation times for motions likely in this polymer. Motions considered include overall rotatory diffusion, three-bond crankshaft motions, anisotropic internal rotation of the phenyl group, and anisotropic internal rotation of the methyl group. According to the interpretation, spin relaxation at high molecular weights is dominated by anisotropic phenyl group rotation characterized by correlation times from 0.2 to 0.4 ns. The three-bond crankshaft motions also contribute to relaxation and the corresponding correlation times range from 1 to 15 ns. The rapid phenyl group rotation accounts for the unusual presence of minima in some of the plots of spin-lattice relaxation times vs. molecular weight. Methyl group rotation is too fast to significantly contribute to relaxation and only serves to partially average the dipole-dipole interactions. The apparent activation energy for phenyl group rotation is 5 kJ, and the apparent activation energy for the three-bond crankshaft motion is 25 kJ. The correlation time for the three-bond crankshaft motion is strongly dependent on concentration while the phenyl group rotational correlation time is only weakly dependent on concentration.

Local motion in poly(2,6-dimethyl-1,4-phenylene oxide) abbreviated here as  $\text{M}_2\text{PPO}$  is expected to be quite different from other polymers recently studied in solution by NMR such as polystyrene,<sup>1-4</sup> polyoxymethylene,<sup>5</sup> and polyisobutylene.<sup>6-9</sup> In polymers containing carbon-carbon single bonds and carbon-oxygen single bonds, backbone rearrangements of the general crankshaft type have been proposed as the dominant local motion although rotation of substituent groups attached to the backbone is also observed.<sup>1-9</sup> In  $\text{M}_2\text{PPO}$ , the backbone is composed of rigid phenyl groups between oxygen atoms and in addition to crankshaft type motions, internal rotation of the phenyl group composing the backbone could be an important local motion.<sup>10</sup> This latter motion has been proposed as the major contributor to the high impact strength of  $\text{M}_2\text{PPO}$ .<sup>10</sup>

To probe local motion in  $\text{M}_2\text{PPO}$ , proton spin relaxation was observed as a function of temperature, concentration, and

molecular weight. The dependence of  $T_1$  of the methyl protons vs. molecular weight served as the primary basis for interpretation. The unusual local chain dynamics in  $\text{M}_2\text{PPO}$  is immediately apparent in the relaxation data since minima are present in the plots of  $T_1$  vs. molecular weight under a variety of experimental conditions. An earlier  $^{13}\text{C}$  NMR study<sup>11</sup> of one high molecular weight sample of  $\text{M}_2\text{PPO}$  found  $T_1$  of all carbons in the repeat unit to be nearly independent of temperature which is also atypical for synthetic polymers in solution. A similar temperature dependence is observed for the  $^1\text{H}$  relaxation times at high molecular weight, and indeed extensive data including molecular weight dependent data are required for the interpretation. The greater sensitivity of  $^1\text{H}$  NMR expedited the acquisition of a large body of data.

The interpretation given here employs a specific motional model presented by Jones and Stockmayer<sup>12</sup> which includes local motions caused by backbone rearrangements and in-

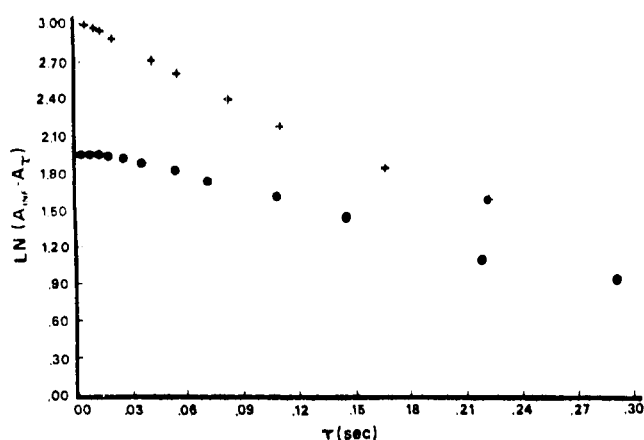


**Figure 1.** The natural logarithm of the quantity given by the signal amplitude after an infinite delay time minus the signal amplitude after a delay time of  $\tau$  plotted vs. delay time. These curves are representative of the decay of the proton magnetizations observed in solutions of  $M_2$ PPO in  $CDCl_3$ . The decay of the methyl proton magnetization is denoted by plus signs and that of the phenyl protons by filled circles.

ternal rotations in addition to a cooperative motion caused by overall rotatory diffusion. The combination of the data with the interpretational model allows for the determination of the time scale, concentration, and temperature dependence of the various motions. The interpretation derived from  $^1H$  relaxation and the specific motional model is checked by predicting the  $T_1$  and NOE of  $^{13}C$  nuclei in  $M_2$ PPO for comparison with the measured values reported at one molecular weight and concentration.<sup>11</sup>

### Experimental Section

High molecular weight samples of  $M_2$ PPO were purchased from Cellomer Associates, Inc. Molecular weight and polydispersity characterization data are provided by the supplier who reports  $M_w = 4.6 \times 10^4$  from a light-scattering determination and  $M_n = 1.7 \times 10^4$  from a gel permeation chromatographic determination. A 40-g sample of this polymer was fractionated from chloroform solution with methanol. Several lots of low molecular weight  $M_2$ PPO were prepared according to the method of Staffin and Price.<sup>13</sup> These lots were fractionated either from 1,2-dichloroethane solution with nitrobenzene or from chloroform solution with methanol.

Solution viscosities of fractions derived from both high and low molecular weight samples were determined in chloroform with an Ubbelohde viscometer suspended in a constant temperature bath regulated at  $25 \pm 0.03^\circ C$ . Couette and kinetic energy corrections were determined on the viscometer by measuring the efflux times of water at several temperatures and were found to be negligible. Viscosity average molecular weights,  $M_v$ , were calculated from the intrinsic viscosity,  $[\eta]$ , according to the equation<sup>14</sup>

$$[\eta](dL/g) = 4.83 \times 10^{-4} M_v^{0.64} \quad (1)$$

The Huggins' constant,  $k'$ , was determined to be 0.55 for  $M_2$ PPO from a plot of specific viscosity vs. concentration for ten concentrations of  $M_2$ PPO in  $CHCl_3$  ranging from 0.0072 to 0.1400 g/mL at  $25 \pm 0.03^\circ C$ .

Fourteen fractions were obtained from the high molecular weight sample with  $M_v$  ranging from  $1.2 \times 10^4$  to  $9.6 \times 10^4$ . The low molecular weight samples typically yield six fractions ranging from  $2.8 \times 10^3$  to  $1.6 \times 10^4$ . These molecular weights are determined with an estimated 5% accuracy. High-resolution proton NMR spectra of all fractions were obtained on a JEOL C60-H high-resolution spectrometer. All spectra were identical with singlets at 2.15 and 6.57 ppm corresponding to the methyl protons and the aromatic protons, respectively.

For the relaxation measurements, solutions of the  $M_2$ PPO fractions in  $CDCl_3$  were prepared by weight in NMR tubes, subjected to five freeze-pump-thaw cycles to remove dissolved oxygen, and sealed under vacuum. Spin relaxation of the methyl protons was observed in a 7 kG field provided by a Bruker 12-in. electromagnet equipped with a five-digit Precision Hall Stabilizer and eight Gradient Electric

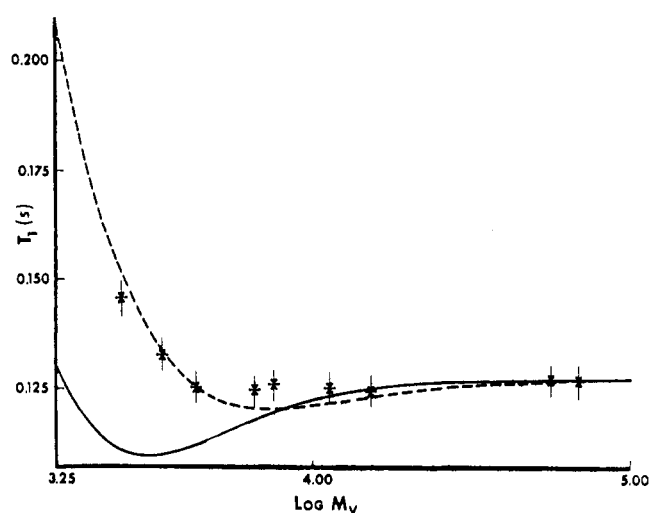


**Figure 2.** Methyl group proton spin-lattice relaxation time  $T_1$  as a function of a molecular weight for 5 wt % solutions of  $M_2$ PPO in  $CDCl_3$  at  $20^\circ C$ . The points are experimental data, and the dashed line is a simulation of the data based on the specific motional model discussed in the interpretation which assumes a polydispersity of  $M_w/M_n = 1.5$  for all fractions. The solid line is a prediction for monodisperse fractions based on the interpretation for polydisperse fractions.

Current Shim Pole Caps, with an NMR Specialties PS 60 pulse console operating at 30 MHz and a Nicolet NMR-812 laboratory computer. A 180- $\tau$ -90 pulse sequence followed by Fourier transformation was used to monitor the return of the two chemically distinct sets of nuclei toward equilibrium. Temperature control was obtained by regulated air or dry  $N_2$  flow through the probe. The out-flow was monitored by means of a chromel-constantan thermocouple and was determined to be within  $1^\circ C$  of the desired temperature of the sample by monitoring the temperature inside an open sample with an additional thermocouple.

### Results

As can be seen in Figure 1, the return of the methyl proton magnetization toward equilibrium is somewhat nonexponential. However, the initial decay is well approximated by a single exponential time constant  $T_1$ , and this constant may be determined by linear least-squares analysis of  $\ln(A_\infty - A_\tau)$  vs.  $\tau$  for short delay times. Specifically linear least-squares analysis yields the same value of  $T_1$  whether delay times extend from 0 to  $T_1/2$  or from 0 to  $T_1$ . However, if delay times ranging from  $\tau = 0$  to  $2T_1$  are considered, the estimate of the initial time constant is systematically increased by 8%. Including delay times from 0 to  $3T_1$  increases the estimate of the initial time constant by 20%. Since no systematic dependence of the estimate of  $T_1$  is observed for delays shorter than one  $T_1$ , the initial time constant will be reported based on six to eight delay times in the range 0 to one  $T_1$ . The initial time constant  $T_1$  will subsequently be identified as the spin-lattice relaxation time of the methyl protons. A typical decay of the magnetization of the phenyl protons is also shown in Figure 1, and it is extremely nonexponential especially at short times. No analysis of the phenyl proton relaxation will be attempted here.

The spin-lattice relaxation time of the methyl protons was measured at  $20^\circ C$  as a function of molecular weight at three concentrations (5, 10, and 20 wt %) shown in Figures 2–4, respectively. The 10% samples were also measured as a function of temperature at 0, 40, and  $70^\circ C$ , shown in Figures 5–7, respectively. A  $T_1$  minimum is seen to appear as the concentration is increased from 5 to 10% and becomes greater as the concentration goes from 10 to 20%. Other results on polymers such as polystyrene<sup>1</sup> and polyisobutylene<sup>7</sup> exhibit no minima as a function of molecular weight and resemble Figures 2, 6,

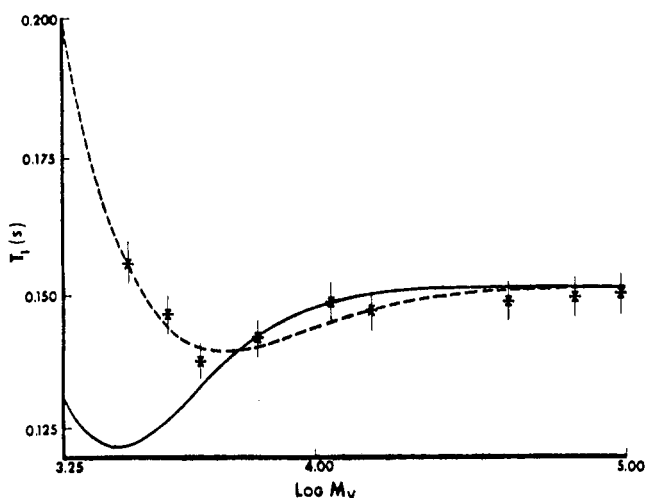


Figure 3. The same plot as Figure 2, but for 10 wt % solutions.

and 7. As the temperature increases and the concentration is held constant the  $T_1$  minimum diminishes until at 70 °C (Figure 7) it is nonexistent. Each point on the plots is the average of two to five separate determinations of  $T_1$  and the typical standard deviation is 3%. The estimated accuracy of the averaged  $T_1$  values is 10%.

### Interpretation

The return of the magnetization to equilibrium in  $M_2PPO$  can be described by the equation of Brooks, Cutnell, Stejskal, and Weiss.<sup>15</sup> For two sets of chemically distinct protons,  $I$  and  $S$ , identified here with methyl and phenyl protons, respectively, the equations are

$$\begin{aligned} -dI/dt &= (n_I \langle \rho_I + \sigma_I \rangle_{av} + n_S \langle \rho \rangle_{av})(I - I_0) \\ &\quad + n_I \langle \sigma \rangle_{av}(S - S_0) \\ -dS/dt &= (n_S \langle \rho_S + \sigma_S \rangle_{av} + n_I \langle \rho' \rangle_{av})(S - S_0) \\ &\quad + n_S \langle \sigma \rangle_{av}(I - I_0) \quad (2) \end{aligned}$$

The two systems are assumed to have only weak indirect spin-spin coupling and in fact only a single signal is observed for each set of chemically distinct nuclei. The number of spins in the  $I$  set is  $n_I$ , and the number of spins in the  $S$  set is  $n_S$ . The transition probabilities caused by dipolar interactions among the protons in set  $I$  are labeled  $\langle \rho_I + \sigma_I \rangle_{av}$ ; the transition probabilities caused by interactions between protons in the  $I$  set and the  $S$  set are labeled  $\langle \rho \rangle_{av}$ ,  $\langle \rho' \rangle_{av}$ , and  $\langle \sigma \rangle_{av}$ ; and the transition probabilities caused by interactions among the protons in set  $S$  are labeled  $\langle \rho_S + \sigma_S \rangle_{av}$ .

The equation for the initial rate of relaxation for set  $I$  can be simplified in the following circumstances. If  $\langle \rho_I + \sigma_I \rangle_{av}$  is much greater than  $\langle \rho \rangle_{av}$  and  $\langle \sigma \rangle_{av}$ , then the equation describing the initial relaxation of the proton set  $I$  reduces to

$$-dI/dt = n_I \langle \rho_I + \sigma_I \rangle_{av}(I - I_0) \quad (3)$$

These circumstances are present in  $M_2PPO$  for the methyl protons if the intramolecular dipole-dipole relaxation mechanism is dominant. The distance between protons within the methyl group is considerably shorter than the average distance between a methyl proton and the nearest phenyl proton. The minus sixth power dependence in the dipole-dipole interaction magnifies the difference resulting in  $\langle \rho_I + \sigma_I \rangle_{av}$  being much greater than  $\langle \sigma \rangle_{av}$  or  $\langle \rho \rangle_{av}$ . The reason eq 3 is only valid initially is the term  $(I - I_0)$  decays more rapidly than  $(S - S_0)$  so eventually  $n_I \langle \rho_I + \sigma_I \rangle_{av}(I - I_0)$  becomes comparable in magnitude to  $n_I \langle \sigma \rangle_{av}(S - S_0)$ . One more factor in favor of the simplification producing eq 3 is the ratio of  $n_I$

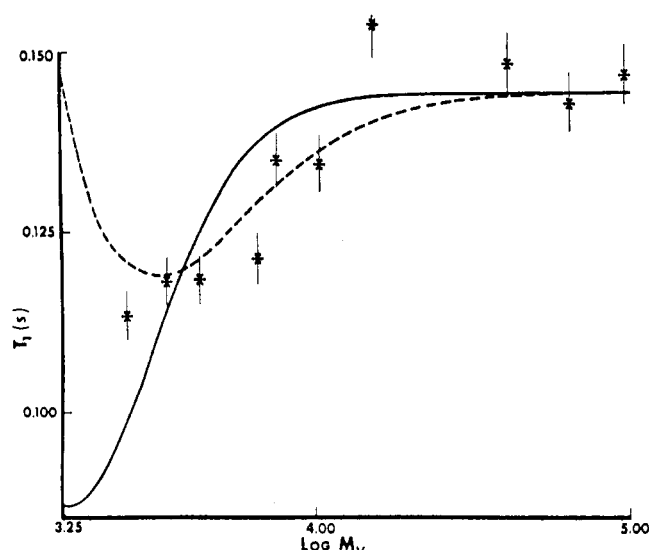


Figure 4. The same plot as Figure 2, but for 20 wt % solutions.

to  $n_S$  which equals 3. This also supports the inequity  $n_S \langle \rho \rangle_{av}$  much smaller than  $n_I \langle \rho_I + \sigma_I \rangle_{av}$ .

No similar simplification is possible with respect to the  $S$  set of protons. In fact all the circumstances which favor a simple first-order rate equation initially for the methyl protons tend to produce a more complicated rate equation for the aromatic protons. This is observed experimentally as shown in Figure 1 where the decay of the magnetization for the aromatic protons is strongly nonexponential especially at short times.

The rate constant in eq 3,  $n_I \langle \rho_I + \sigma_I \rangle_{av}$ , can be identified<sup>15</sup> with the equations described by Solomon<sup>16</sup> for  $1/T_1$  in terms of spectral densities,  $J$ , if the intramolecular dipole-dipole relaxation mechanism is dominant and correlation effects are neglected.

$$\begin{aligned} 1/T_1 &= n_I \langle \sigma_I + \rho_I \rangle_{av} = \sum_j \left( \frac{9}{8} \right) \gamma^4 \hbar^2 r_j^{-6} (J_1(\omega_H) \\ &\quad + J_2(2\omega_H)) \quad (4) \end{aligned}$$

The proton gyromagnetic ratio is denoted by  $\gamma$ , the Larmor frequency by  $\omega_H$ , and the internuclear separation in the methyl group by  $r$ . The motion of protons in the methyl group is certainly correlated and the relaxation in such a case can also be nonexponential even in the absence of any interactions with a second set of spins. Correlation effects have been considered theoretically in detail by Werbelow, Grant, and Marshall<sup>17-20</sup> with the conclusion that correlation effects could be significant in a system similar to  $M_2PPO$ . However, they also point out that the initial rate of decay is approximated by eq 4, and thus observation of the initial rate of decay minimizes complications caused both by cross-relaxation and correlation.

It therefore is reasonable to identify the initial rate of decay summarized graphically in Figures 2-7 with spectral densities according to eq 4. This approach fulfills the present goal of characterizing local motion in  $M_2PPO$  from the relaxation of the methyl spin system. To check the validity of this approach, the interpretation based on the initial rate will be compared with  $^{13}C$  relaxation data free from cross-relaxation and correlation effects. A complete characterization of proton relaxation in  $M_2PPO$  including and accounting for both cross-relaxation and correlation is left for future consideration.

To relate the proton spin relaxation to motions likely in a randomly coiled chain, the model of Jones and Stockmayer<sup>12</sup> will be used. Three general classes of overall motion are con-

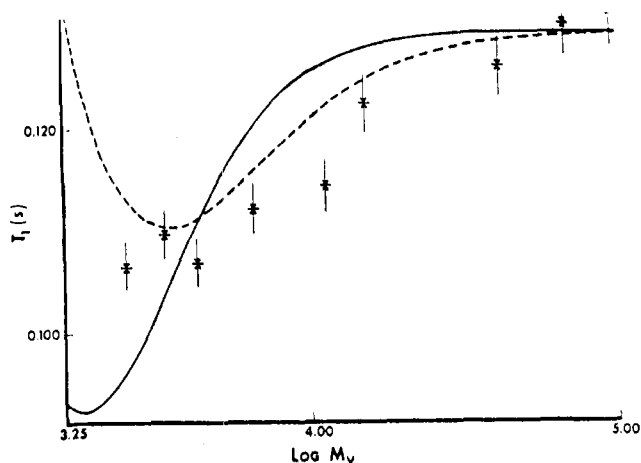


**Figure 5.** Methyl group proton spin-lattice relaxation time  $T_1$  as a function of molecular weight for 10 wt % solutions of  $M_2PPO$  in  $CDCl_3$  at 0 °C. The solid and dashed lines have the same significance as Figure 2.

sidered in this model: (1) overall rotatory diffusion, (2) backbone rearrangements caused by the three-bond motion, and (3) internal anisotropic rotation relative to the backbone bonds. Each of these motions is considered as an independent source of motional modulation of the dipole-dipole interaction so that the combined correlation function is just a product of the correlation functions associated with each motion.

Overall rotatory diffusion can be characterized by a simple exponential correlation function. The correlation time at infinite dilution,  $\tau_0'$ , can be estimated with confidence from the molecular weight  $M$  and the intrinsic viscosity  $[\eta]$  of the polymer in a given solvent of viscosity  $\eta_0$ .

$$\tau_0' = 2M[\eta]\eta_0/3RT \quad (5)$$

The expression for the correlation time is based on a rotatory diffusion coefficient for a rigidly rotating spherically symmetric random coil.<sup>21,22</sup> In solution of finite concentration, the overall rotatory diffusion time will be estimated from eq 6 which is analogous to the Martin variation of the Huggins equation for specific viscosity.

$$\ln(\tau_0/\tau_0') = k'[\eta]c \quad (6)$$

An equation of this form has also been employed by others to interpret the low-frequency dielectric dispersion attributed to cooperative chain motions.<sup>23,24</sup> As mentioned earlier, the constant  $k'$  was fixed at 0.55 by fitting steady-flow reduced viscosity over a concentration range comparable to that of the NMR study.

In polydisperse samples, there will not be a single correlation time for rotatory diffusion but rather a distribution of correlation times determined by the distribution of molecular weights. The effects of a molecular weight distribution can be introduced by folding a Schulz-Zimm molecular weight distribution function with the correlation function containing  $\tau_0$  written explicitly as a function of molecular weight.<sup>4</sup> The ratio of  $M_w/M_n$  is not known for each of the fractions studied. However, in the unfractionated high molecular weight sample,  $M_w/M_n$  was determined by the manufacturer to be 2.7, and this sample was separated into 14 fractions ranging in molecular weight from  $1.2 \times 10^4$  to  $9.6 \times 10^4$ . It is likely that  $M_w/M_n$  of the fractions lies in the range 1.33 to 2.0 so a value of 1.5 will be used as an estimate for all fractions studied. Errors introduced by relying on only an estimate of  $M_w/M_n$  will be mentioned later.

The second independent motion is backbone rearrangement caused by the action of the three-bond jump in a chain lying

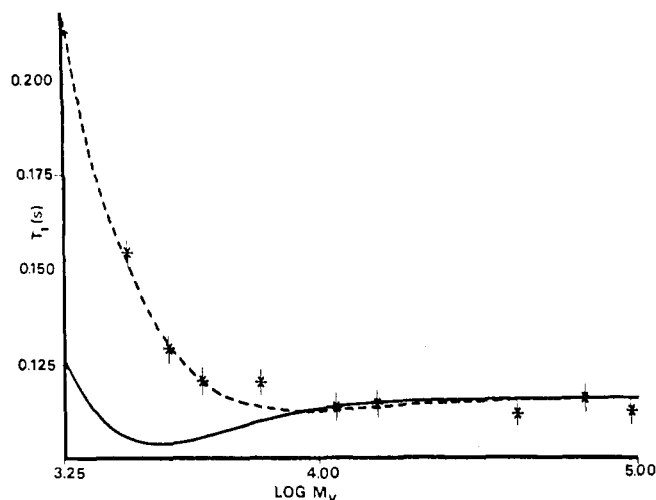


**Figure 6.** The same plot as Figure 5, but at 40 °C.

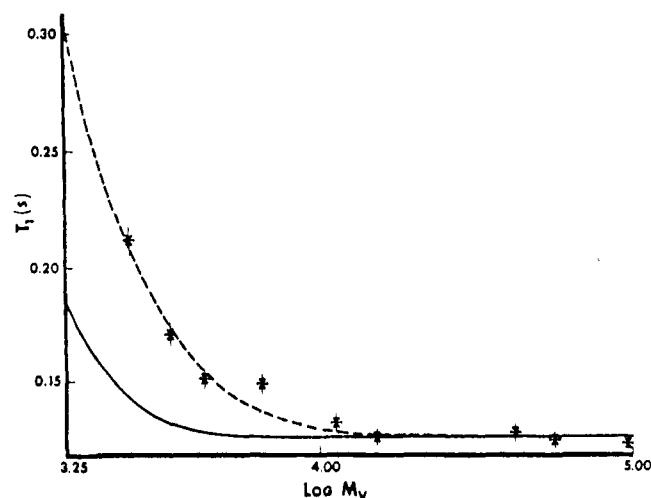


**Figure 7.** The same plot as Figure 5, but at 70 °C.

on a tetrahedral lattice.<sup>25,26</sup> This description of backbone motion is only applicable to a chain lying approximately on a tetrahedral lattice,<sup>25,26</sup> and the backbone in  $M_2PPO$  is composed of rigid phenyl groups between oxygen atoms with an angle between phenyl groups not greatly different from 109°. The sharp cutoff model<sup>12</sup> for three-bond jumps within a finite segment of chain containing  $2m - 1$  bonds embedded in a larger chain yields the correlation function  $\Phi(t)$  given below for  $(3 \cos^2 \theta - 1)/2$ .

$$\begin{aligned} \Phi(t) &= \sum_{k=1}^s G_k \exp(-t/\tau_k) \\ s &= (m + 1)/2 \\ \tau_k^{-1} &= w \lambda_k \\ \lambda_k &= 4 \sin^2 \left( \frac{k\pi}{2(m + 1)} \right) \end{aligned} \quad (7)$$

The distribution of correlation times  $\tau_k$  characterizes backbone motion in this model and it is convenient to summarize the distribution by the harmonic mean,  $\tau_h$ , and the simple average  $\tau_a$ .

$$\begin{aligned} \tau_h &= \langle \tau_k^{-1} \rangle^{-1} \\ \tau_a &= \langle \tau_k \rangle \end{aligned} \quad (8)$$

The distribution of correlation times and the average values are determined by the rate of occurrence of the three-bond

jump,  $w$ , and the number of bonds,  $2m - 1$ , in the finite segment. The weighting factors in the distribution,  $G_k$ 's, are for the case of "no backsteps" on the lattice.<sup>12</sup>

The last motions to be considered are anisotropic internal rotations relative to the backbone bonds which in the present case are the virtual bonds between oxygen atoms in place of the rigid phenyl groups. Two internal rotations are conceivable: phenyl group rotation about the  $C_1C_4$  axis and methyl group rotation about the threefold symmetry axis. Both of these motions take place in a coordinate system clearly defined relative to the virtual bonds of the backbone as shown in Figure 9. The  $C_1C_4$  axis direction which is also the virtual bond direction is labeled  $z'$ , and the threefold methyl axis direction is labeled  $z''$ . The angle between these two directions is  $\Delta = 60^\circ$ , and the angle between the proton internuclear vector within the methyl group and the  $z''$  axis is  $\alpha = 90^\circ$ .

Following the development by Woessner<sup>27</sup> and others,<sup>11,28</sup> the two internal rotations are combined in the Appendix with isotropic motion caused by backbone rearrangements and overall rotatory diffusion to produce a correlation function. Phenyl group rotation is described by random jumps between two energetically equivalent equilibrium positions at  $\phi'$  and  $\phi' \pm \pi$  at an average rate of  $(2\tau_{irp})^{-1}$ . Methyl group rotation is described by random jumps among three equivalent positions at  $\phi''$  and  $\phi'' \pm 2\pi/3$  at an average rate of  $(3\tau_{irm})^{-1}$ . Methyl group rotation in  $M_2PPO$  is known<sup>29,30</sup> to be rather fast since it undergoes nearly free rotation on the NMR time scale in the solid down to temperatures below  $-200^\circ\text{C}$ . The  $T_1$  minimum<sup>30</sup> yields an estimate of the correlation time for methyl group rotation of  $10^{-9}$  s in the solid at about  $-200^\circ\text{C}$ . If the correlation time  $\tau_{irm}$  in solution is more than two orders of magnitude shorter than the other correlation times, a simplified form of the correlation function and spectral density is appropriate.<sup>31</sup> The correlation times in  $M_2PPO$  in solution at room temperature can be estimated from  $T_1$  to be in the range of  $10^{-10}$  to  $10^{-9}$  s using the simple isotropic motional model. If a correlation time for methyl group rotation of the order of  $10^{-9}$  s is observed in the solid at  $-200^\circ\text{C}$ , it is reasonable to assume that in solution at room temperature it is more than two orders of magnitude shorter. Therefore the simplified expressions for the correlation function and spectral density derived in the Appendix will be employed.

The spectral densities arising from overall rotatory diffusion, backbone rearrangements, phenyl group rotation, and rapid methyl group rotation are

$$J_i = 2fK_i \sum_{k=1}^s \frac{A'\tau_{k0}}{1 + \omega_i^2\tau_{k0}^2} + \frac{B'\tau_{bk0}}{1 + \omega_i^2\tau_{bk0}^2} + \frac{C'\tau_{k0}}{1 + \omega_i^2\tau_{k0}^2} \quad (9)$$

$\tau_{bk0}^{-1} = \tau_0^{-1} + \tau_k^{-1} + \tau_{irp}^{-1}$ ;  $\tau_{k0}^{-1} = \tau_0^{-1} + \tau_k^{-1}$ ;  $A' = (3 \cos^2 \Delta - 1)^2/4$ ;  $C' = (3 \sin^4 \Delta)/4$ ;  $B' = (3 \sin^2 2\Delta)/4$ ;  $f = (3 \cos^2 \alpha - 1)^2/4 = 1/4$ ;  $K_0 = 4/5$ ;  $K_1 = 2/15$ ; and  $K_2 = 8/15$ . The spectral densities have no dependence upon  $\tau_{irm}$  but the dipolar interactions have been reduced by the factor  $(3 \cos^2 \alpha - 1)^2/4$ . This factor has previously been proposed for cases of rapid internal anisotropic rotation.<sup>31</sup>

To determine the correlation times corresponding to backbone motion and phenyl group rotation in  $M_2PPO$  in solution, the molecular weight dependence of  $T_1$  at a given temperature and concentration is simulated from eq 4 and 9. The parameters of the simulation are  $\tau_{irp}$ ,  $w$  or equivalently  $\tau_h$ , and the number of bonds,  $2m - 1$ , in the finite segment of chain. The correlation time for overall rotatory diffusion,  $\tau_0$ , is entered as a known calculated from eq 5 and 6, and the molecular weight distribution is described by a Schulz-Zimm function with  $M_w/M_n = 1.5$  for all fractions. A value of  $1.77 \text{ \AA}$  is used for the proton separation in the methyl group. The simulations of  $T_1$  vs. molecular weight are shown in Figures 2-7 as a dashed line and the correlation times producing these curves are given in Table I. The solid line in these figures is

**Table I**  
Simulation Parameters Characterizing Local Motion in  $M_2PPO$

Concn, wt % in $\text{CDCl}_3$	$T$ , $^\circ\text{C}$	$\tau_{irp}$ , ns	$\tau_h$ , ns	$2m - 1$	$T_1$ , s (high mol wt limit)
5	20	0.19	3.0	5	0.126
10	20	0.29	5.3	5	0.122
20	20	0.41	13	5	0.147
10	0	0.35	9.6	5	0.141
10	20	0.29	5.3	5	0.122
10	40	0.25	2.3	5	0.113
10	70	0.21	1.1	5	0.118

the prediction for monodisperse samples based on the correlation times determined with the inclusion of a Schulz-Zimm molecular weight distribution.

Several points concerning the simulation should be made. As seen from Table I, the model is able to sensibly account for all the data. The correlation times shorten with increasing temperature and lengthen with increasing concentration. The dip or minima observed in some of the experimental plots of  $T_1$  vs. molecular weight can be simulated, and indeed the unusual shape of the curves aids in the determination of the simulation parameters. The finite segment length controlling the extent of coupling of the motion of backbone bonds is the same for all simulations. Only two parameters,  $\tau_{irp}$  and  $\tau_h$ , change as a function of concentration and temperature.

Attempts were made to interpret the data with several other models. A simple Woessner model<sup>27</sup> allowing for overall rotatory diffusion, internal rotation of the methyl group, and internal rotation of the phenyl group could not account for the data. The failure of a model including only internal rotations and overall rotatory diffusion has been discussed earlier,<sup>3,4</sup> and similar inconsistencies were encountered in this application as well. The failure of the internal rotation model implies the crankshaft motions described here by the three-bond jump play an important role in spin relaxation. However, if a simulation is attempted based only on a model including fast methyl group rotation, overall rotatory diffusion, and a distribution of correlation times to characterize backbone motion without phenyl group rotation, the data presented in Figures 2-7 cannot be rationalized. To present an example of this, the proton spin relaxation in 10% solutions at  $20^\circ\text{C}$  is simulated with the model presented here except that phenyl group rotation is not allowed. The "best" fits shown in Figure 8 are obtained by fitting  $T_1$  in the high molecular weight limit. At low molecular weights, consistent discrepancies of 30% arise which is well beyond experimental error. Note that a minimum is produced in one of the "best" fits in Figure 8 involving a correlation time on the far side of the  $T_1$  minimum from the extreme narrowing limit. However, the fit is very poor, and other relaxation parameters calculated from this fit such as the  $^{13}\text{C}$  NOE are far from experimentally observed values. Although minima in plots of  $T_1$  vs. molecular weight are found for very slow local motions in competition with overall rotatory diffusion, simplistic estimates<sup>11</sup> as well as the detailed analysis presented here indicate dominant motions with correlation times in the range of  $10^{-10}$  to  $10^{-9}$  s. For this time scale and in our hands, the inclusion of an anisotropic motion is required to simulate the shapes of the observed curves including minima or downward trends in  $T_1$  with decreasing molecular weight.

In the description employed here based on the three-bond jump, backbone motion is characterized by a sum over several exponential correlation times. The distribution is controlled by the choice of segment length for coupling. Other models with various distributions of correlation times for backbone motion have also been considered, but they too produce sim-

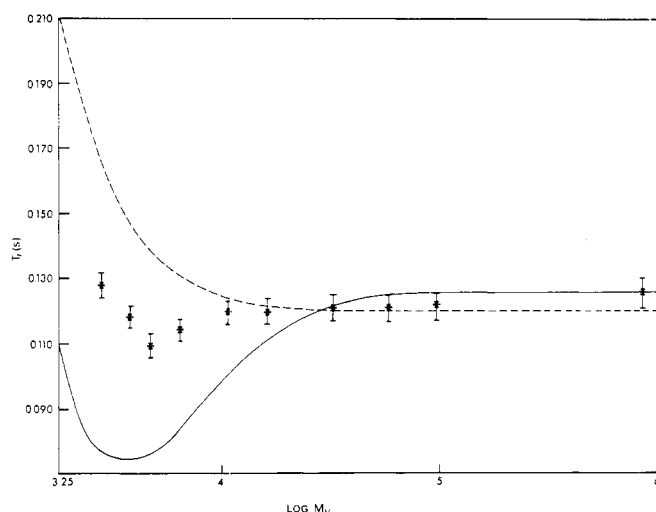


**Figure 8.** Methyl group proton spin-lattice relaxation time  $T_1$  as a function of molecular weight for a 10 wt % solution of  $M_2$ PPO in  $CDCl_3$  at 20 °C. Both curves are “best” simulations when only three-bond jumps and fast methyl group rotation are included as local motions. Phenyl group rotation is specifically excluded. Both curves include the effects of a molecular weight distribution with  $M_w/M_n = 1.5$ . The upper dashed curve is produced with  $\tau_h = 0.3$  ns which is on the extreme narrowing side of the  $T_1$  minimum. The lower curve is produced with  $\tau_h = 15$  ns which is on the far side of the  $T_1$  minimum from the extreme narrowing limit. The parameter  $s$  controlling the distribution of correlation times is set at 2 for both curves although the shape of the curves is not a strong function of the breadth of the distribution. Neither curve is a satisfactory simulation.

ulations of the quality shown in Figure 8. The defect diffusion model<sup>25,26</sup> is among these, and it has been shown to be incapable of simulating relaxation in other cases.<sup>4</sup> When the defect diffusion model is modified by the inclusion of an additional exponential correlation time,<sup>12,25,26</sup> a correlation function is obtained which is nearly mathematically identical with the one employed here for backbone motion<sup>4,12</sup> and it too is found deficient in this application if phenyl group rotation is not included. The failure of these simulation attempts implies that phenyl group rotation is a key component of the interpretation.

The defect diffusion model with the inclusion of an additional exponential correlation time<sup>4,25,26</sup> could just as well have been combined with phenyl group rotation as the description of backbone motion used here, but we prefer the “sharp cut-off” model for reasons discussed elsewhere.<sup>12</sup>

The most versatile of the distribution of correlation time models is based on a logarithmic  $\chi^2$  or  $\gamma$  distribution of correlation times.<sup>32</sup> The distribution of correlation times may be spread over several orders of magnitude in time, and the model has been successful in interpreting relaxation in polymers dominated by backbone rearrangement. This local motion model was combined with overall rotatory diffusion and a molecular weight distribution with  $M_w/M_n = 1.5$  in an attempt to interpret the data presented here. However, in our hands, no satisfactory simulation of the data in Figures 4 and 5 was found with  $b = 10, 100$ , or 1000 and any choice of  $p$  and  $\bar{\tau}$ . The downward trend in  $T_1$  with decreasing molecular weight could not be matched for choices of parameters that also reproduced  $T_1$  in the high molecular weight limit. Most commonly,  $T_1$  was systematically higher or lower over some range of molecular weights similar to the poor simulation shown in Figure 8. Possibly a broader distribution of correlation times than can be achieved with  $b = 10, 100$ , or 1000 could provide a basis for a simulation. However, the distribution with  $b = 1000$  and  $p = 2$  is already considerably broader than those reported for other polymer systems.<sup>32</sup>

The higher temperature and lower concentration curves with shallow minima or no minima can be simulated with the  $\chi^2$  model but the parameters of the simulation are not physically sensible. A good fit to the data of Figure 3 at 20 °C is achieved with  $b = 1000$ ,  $p = 2$ , and  $\bar{\tau} = 1.6 \times 10^{-11}$  s while a good fit to the data of Figure 6 at 40 °C is achieved with  $b = 1000$ ,  $p = 6$ , and  $\bar{\tau} = 2.3 \times 10^{-11}$  s. These distributions are extremely broad and in fact are even broader than those reported for rubbery solids.<sup>32</sup> Second the “average” or characteristic correlation time  $\bar{\tau}$  lengthens as temperature increases in opposition to common expectation and such behavior precludes an estimation of an apparent activation energy. The breadth parameter is very strongly temperature dependent as can be seen from the two cases presented here. Again the physical significance of this result is unclear unless viewed from the earlier interpretation based on specific motions. In that model there are three distinct local motions of rather different time scale. They are backbone rearrangement with a correlation time of  $10^{-8}$  to  $10^{-9}$  s, phenyl group rotation with a correlation time of  $10^{-10}$  s, and methyl group rotation with a correlation time of about  $10^{-12}$  s. At higher temperatures, the spread between these correlation times is smaller but it increases as temperature is lowered mainly because the backbone motion is associated with a high activation energy and slows rapidly. An increasing separation between the phenyl group rotational correlation time and the backbone correlation time can be seen in Table I. The growing spread in correlation times with decreasing temperature is reflected by decreases in  $p$  apparent in the two examples. In our opinion, the very broad distribution and the temperature dependence of the breadth reflect difficulties associated with interpreting dynamics involving several distinct motions with a model employing a continuous distribution of correlation times.

An interpretation is possible if the  $\chi^2$  distribution is used to describe only backbone motion and methyl and phenyl group rotation are added. However, it is necessary to assume that the motion described by each correlation time in the  $\chi^2$  distribution is simple isotropic tumbling of the repeat units even though conformational changes must be more complicated. Without this assumption, it is not possible to specify the geometric relationship between internal rotation and backbone motions since the latter are not based on a structurally specific description of backbone motion in the  $\chi^2$  model. Again the use of backbone description based on the three-bond model is preferred for this reason and others discussed elsewhere.<sup>12</sup>

No interpretation would have been possible if  $T_1$  had only been measured at a high molecular weight. An inspection of  $T_1$  in the high molecular weight limit given in Table I shows only very slight and nonmonotonic changes with temperature and concentration. Actually according to the interpretation given here, room temperature is near a broad minimum of  $T_1$  vs. temperature.

A check on all aspects of the interpretation involving specific motions can be made by predicting the  $T_1$  and NOE of  $^{13}C$  nuclei in  $M_2$ PPO based on the correlation times determined from proton relaxation. Laupretre and Monnerie<sup>11</sup> have determined  $^{13}C$  relaxation parameters on the 3 and 5 carbons of the phenyl ring for 10 vol %  $M_2$ PPO in  $CDCl_3$  at 30 °C in a 23.5 kG field. These conditions of temperature and concentration do not precisely coincide with any of our experimental conditions so it is necessary to interpolate to obtain the corresponding correlation times. With the model and the interpolated correlation times,  $T_1$  and the NOE are predicted to be 85 ms and 1.9, respectively, while Laupretre and Monnerie report 93 ms and 1.6.<sup>11</sup> The agreement is very good and supports the interpretation. In particular, the identification of the initial rate with  $T_1$ , the neglect of correlation effects, and

the assumption of rapid methyl group rotation are unlikely to be in serious error since none of these factors affected the relaxation parameters of  $^{13}\text{C}$  nuclei in the 3 and 5 position.

If the interpretation is assumed to be reasonable, the precision of the determination of the simulation parameters is worthy of consideration. The estimates of the precision given here are based on the sensitivity to variation observed during the simulation process. The number of bonds in the finite segment determining the coupling of backbone motion is either 5 or 7, but 5 does give a better simulation. The correlation times  $\tau_h$  and  $\tau_{irp}$  vary as much as  $\pm 30\%$  depending upon the choice of segment length, the choice of the internuclear distance, and the choice of the molecular weight distribution. A change in internuclear separation of  $0.01 \text{ \AA}$  is about equivalent to a 10% change in  $T_1$ . The internuclear separation is known no better than  $\pm 0.01 \text{ \AA}$  so a discrepancy of 10 or 20% between the observed and predicted  $^{13}\text{C}$   $T_1$ 's and NOE is conceivable. The initial report<sup>33</sup> of proton spin relaxation in  $\text{M}_2\text{PPO}$  based the interpretation on a description of backbone motion allowing backsteps which again causes changes in the values of the correlation times of  $\pm 30\%$ . Varying the choice of the molecular weight distribution used in the simulations between 1.33 and 2.00 does not result in an uncertainty greatly different from the others inherent in the simulation so we shall be content with utilizing only an estimate of the polydispersity. However, once a choice of all model parameters aside from correlation times is made, the variation in  $\tau_{irp}$  and  $\tau_h$  is somewhat reduced. In the curves with minima, only a small range of  $\tau_{irp}$  and  $\tau_h$  produces reasonable simulations, but for curves which are monotonic such as the  $70^\circ\text{C}$  data the uncertainty in  $\tau_{irp}$  and  $\tau_h$  again approaches 30%.

## Discussion

The spin relaxation data on  $\text{M}_2\text{PPO}$  in solution are accounted for in terms of two distinct local motions of rather different time scales. The dependence of  $T_1$  on molecular weight is unusual with the presence of  $T_1$  minima under several experimental conditions. According to the interpretation, this unusual behavior reflects the domination of relaxation by internal rotation of the phenyl group. Phenyl group rotation is roughly an order of magnitude faster than backbone rearrangements caused by crankshaft type motions. The presence of such minima has been predicted earlier<sup>34</sup> for cases of internal rotation in competition with overall rotatory diffusion, but this is the only known report of such behavior for a randomly coiled macromolecule in solution.

The concentration dependence of the correlation times characterizing phenyl group rotation and backbone rearrangement are also quite different. The average correlation time for backbone motion changes much more rapidly with concentration than the correlation time for phenyl group rotation. This is plausible since the basic backbone rearrangement is the concerted movement of three phenyl groups while phenyl group rotation involves only a single unit.

An apparent activation energy can be calculated for backbone rearrangements and for phenyl group rotation. The apparent activation energy of backbone rearrangements determined from the temperature dependence of  $\tau_h$  is  $25 \text{ kJ}$  compared with  $5 \text{ kJ}$  for phenyl group rotation determined from the temperature dependence of  $\tau_{irp}$ . The low value for the barrier for phenyl group rotation is in general agreement with the semiempirical calculations of Tonelli.<sup>10,35</sup> However, the barrier to rotation has also been calculated by Laupretre and Monnerie<sup>36</sup> and found to be about three times larger than the value determined from the spin relaxation data or the calculation of Tonelli.<sup>10,35</sup> The calculation by Laupretre and Monnerie<sup>36</sup> combined with the lack of a dependence of  $T_1$  on temperature<sup>11</sup> has led these authors to suggest that rotation

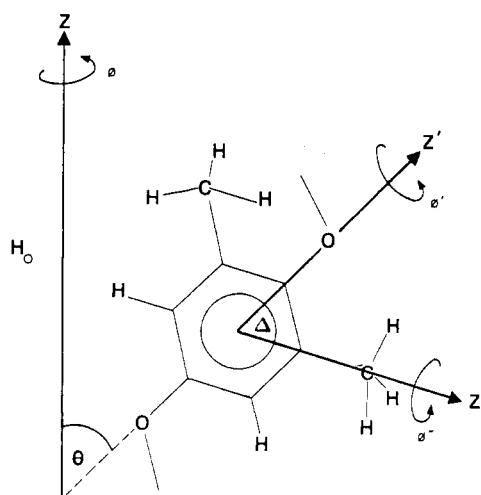


**Figure 9.** A monomer unit of  $\text{M}_2\text{PPO}$  represented in a coordinate system defined relative to the virtual bonds of the backbone. The  $z'$  and  $z''$  axes are the axes of internal rotation of the phenyl group and methyl group, respectively, separated by the angle  $\Delta = 60^\circ$ . The variable azimuth of  $z''$  and  $z'$  is denoted by  $\phi'$  and the variable azimuth of an internuclear proton vector of the methyl group about the  $z''$  axis is denoted by  $\phi''$ . The angle between the  $z'$  axis and the external magnetic field  $H_0$  is  $\theta$  with  $\phi$  denoting the azimuthal angle. The angle between the  $z''$  axis and the proton-proton internuclear vector is  $\alpha = 90^\circ$  and is not shown in this figure.

of the phenyl group does not occur but only oscillation. However, a quantitative interpretation of  $T_1$  based on oscillatory motions was not presented. To add to the dilemma, Schaefer, Stejskal, and Buchdahl<sup>37</sup> observed two resonances for the 3 and 5 phenyl carbons in solid  $\text{M}_2\text{PPO}$ . This is interpreted in terms of an absence of phenyl group rotation although some oscillation is still supposed to be present in the solid.<sup>38</sup> The only apparent reconciliation of the interpretation of the solution data presented here and solid NMR data lies in domination and restriction of phenyl group motion in the solid by intermolecular effects. Experiments in solution are being extended to higher concentration to determine if phenyl group rotation is reduced at high concentration. The proposed reconciliation of the NMR data in solution and the solid does not resolve the interpretational discrepancy between this work and that of Laupretre and Monnerie.<sup>11,36</sup>

It is also informative to compare the results of the interpretation presented here for  $\text{M}_2\text{PPO}$  with the only other polymer containing phenyl groups for which considerable relaxation data are available, polystyrene.<sup>1-4</sup> In polystyrene, the dominant motion causing spin relaxation is backbone rearrangements with internal rotation of the phenyl group making only minor contributions.<sup>28</sup> According to the sharp cutoff model,<sup>12</sup> the coupling of motion associated with the three-bond jump extends over a somewhat greater number of bonds in polystyrene<sup>4</sup> but in both polymers the number is in the range of 5 to 15. The correlation<sup>3,4,28</sup> times for backbone motion and phenyl group rotation in polystyrene are approximately equal<sup>28</sup> with the correlation time for internal rotation only somewhat longer even though it contributes little to spin relaxation. This is just the reverse of the interpretation presented for  $\text{M}_2\text{PPO}$ , and it is attractive to associate the unusual properties of solid  $\text{M}_2\text{PPO}$  with the unusual local chain dynamics observed in solution.<sup>10,35</sup> Before this can be done in a definitive manner, the question of restricted rotation must be further clarified.

**Acknowledgment** is made to the donors of the Petroleum Research Fund, administered by the American Chemical Society, for the support of this research. Equipment obtained



under National Science Foundation Equipment Grant No. GP29185 was utilized in this research. One of us (R.P.L.) also thanks Lever Brothers Foundation for partial support.

## Appendix

Following the development of Woessner,<sup>27</sup> the spectral density can be written in terms of the Fourier transformation of the orientation functions at frequency  $\omega$ .

$$J_i(\omega) = \int_{-\infty}^{\infty} \langle F_i^*(t) F_i(0) \rangle \exp(i\omega t) dt \quad (\text{A1})$$

The orientation functions are

$$\begin{aligned} F_0(t) &= (1 - 3z^2) \\ F_1(t) &= (x + iy)z \\ F_2(t) &= (x + iy)^2 \end{aligned} \quad (\text{A2})$$

where  $x, y, z$  are the direction cosines of the internuclear vector with respect to a laboratory coordinate system. Note that  $\langle F_i^*(t) F_i(0) \rangle$  is a correlation function similar to eq 7 aside from constants.

Using trigonometry and the geometry in Figure 9, the direction cosines can be expressed in terms of the angles  $\phi, \theta, \phi', \phi'', \Delta$ , and  $\alpha$ .

$$\begin{aligned} \begin{vmatrix} x \\ y \\ z \end{vmatrix} &= \begin{vmatrix} \cos \theta \cos \phi & -\sin \phi & \sin \theta \cos \phi \\ \cos \theta \sin \phi & \cos \phi & \sin \theta \sin \phi \\ -\sin \theta & 0 & \cos \theta \end{vmatrix} \begin{vmatrix} x' \\ y' \\ z' \end{vmatrix} \\ \begin{vmatrix} x' \\ y' \\ z' \end{vmatrix} &= \begin{vmatrix} \cos \Delta \cos \phi' & -\sin \phi' & \sin \Delta \cos \phi' \\ \cos \Delta \sin \phi' & \cos \phi' & \sin \Delta \sin \phi' \\ -\sin \Delta & 0 & \cos \Delta \end{vmatrix} \begin{vmatrix} x'' \\ y'' \\ z'' \end{vmatrix} \\ \begin{vmatrix} x'' \\ y'' \\ z'' \end{vmatrix} &= \begin{vmatrix} \sin \alpha \cos \phi'' \\ \sin \alpha \sin \phi'' \\ \cos \alpha \end{vmatrix} \end{aligned} \quad (\text{A3})$$

For instance the expression for  $z$  is

$$\begin{aligned} z &= -\sin \theta (\cos \Delta \cos \phi' \sin \alpha \cos \phi'' - \sin \phi' \sin \alpha \sin \phi'' \\ &\quad + \sin \Delta \cos \alpha \cos \phi') + \cos \theta (-\sin \Delta \sin \alpha \cos \phi'' \\ &\quad + \cos \Delta \cos \alpha) \end{aligned} \quad (\text{A4})$$

Substituting into eq A2 for  $F_0(t)$  with  $\alpha = 90^\circ$  yields

$$\begin{aligned} F_0(t) &= 1 - 3z^2 = 1 - 3 \sin^2 \theta \cos^2 \Delta \cos^2 \phi' \cos^2 \phi'' \\ &\quad - 3 \sin^2 \theta \sin^2 \phi' \sin^2 \phi'' \\ &\quad + 6 \sin^2 \theta \cos \Delta \cos \phi' \sin \phi' \cos \phi'' \sin \phi'' \\ &\quad - 3 \cos^2 \theta \sin^2 \Delta \cos^2 \phi'' \\ &\quad - 6 \sin \theta \cos \theta \cos \Delta \sin \Delta \cos \phi' \cos^2 \phi'' \\ &\quad + 6 \sin \theta \cos \theta \sin \Delta \sin \phi' \cos \phi'' \sin \phi'' \\ &= \sum_i f_i(t) g_i(t) h_i(t) \end{aligned} \quad (\text{A5})$$

where  $f_1 = 1; f_2 = -3 \cos^2 \Delta \sin^2 \theta(t); f_3 = -3 \sin^2 \theta(t); f_4 = 6 \cos \Delta \sin^2 \theta(t); f_5 = -3 \sin^2 \Delta \cos^2 \theta(t); f_6 = -6 \sin 2\Delta \sin 2\theta(t)/4; f_7 = 6 \sin \Delta \sin \theta(t) \cos \theta(t); g_1 = 1; g_2 = \cos^2 \phi'(t); g_3 = \sin^2 \phi'(t); g_4 = \cos \phi'(t) \sin \phi'(t); g_5 = 1; g_6 = \cos \phi'(t); g_7 = \sin \phi'(t); h_1 = 1; h_2 = \cos^2 \phi''(t); h_3 = \sin^2 \phi''(t); h_4 = \cos \phi''(t) \sin \phi''(t); h_5 = \cos^2 \phi''(t); h_6 = \cos^2 \phi''(t); and  $h_7 = \cos \phi''(t) \sin \phi''(t)$ . The angles  $\phi, \theta, \phi',$  and  $\phi''$  are time dependent in the motional model and under the assumption of the independence of each motion, the time dependent averages in the calculation of  $\langle F_i(t) F_i(0) \rangle$  can be separated into three averages: one over  $\theta$  and  $\phi$ , the second over  $\phi'$ , and the third over  $\phi''$ . Under these conditions,  $\langle F_0(t) F_0(0) \rangle$  can be written as$

$$\langle F_0(t) F_0(0) \rangle = \sum_{i=1}^7 \sum_{k=1}^7 \langle f_i(t) f_k(0) \rangle \langle g_i(t) g_k(0) \rangle \langle h_i(t) h_k(0) \rangle \quad (\text{A6})$$

The time dependence of  $\theta$  and  $\phi$  results from the isotropic motions of the phenyl group and is characterized by the product of the correlation functions for overall rotatory diffusion given by a single exponential and for backbone rearrangements given by eq 7. For instance,

$$\begin{aligned} \langle \cos^2 \theta(t) \cos^2 \theta(0) \rangle &= \exp(-t/\tau_0) (1/5) \sum_{k=1}^s G_k \exp(-t/\tau_k) \\ &= (1/5) \sum_{k=1}^s G_k \exp(-t/\tau_{k0}) \quad (\text{A7}) \\ \tau_{k0}^{-1} &= \tau_k^{-1} + \tau_0^{-1} \end{aligned}$$

The time dependence of  $\phi'$  in this model is caused by the rotation of the phenyl group about the  $C_1C_4$  axis. This motion will be assumed to be caused by random jumps between two energetically equivalent equilibrium positions at  $\phi'$  and  $\phi' \pm \pi$  at an average rate of  $(2\tau_{\text{irp}})^{-1}$ . This description of motion has been used previously<sup>28</sup> to obtain the time averages involving  $\phi'$  needed for the evaluation of  $\langle F_0(t) F_0(0) \rangle$ . They are

$$\begin{aligned} \langle \exp(\pm i\phi'(0)) \exp(\mp i\phi'(t)) \rangle &= \exp(-t/\tau_{\text{irp}}) \\ \langle \exp(\pm 2i\phi'(0)) \exp(\mp 2i\phi'(t)) \rangle &= 1 \end{aligned} \quad (\text{A8})$$

The time dependence of  $\phi''$  in this model is caused by the rotation of the methyl group about the threefold symmetry axis. If this process takes place by random jumps among three equivalent positions at  $\phi''$  and  $\phi'' \pm 2\pi/3$  at an average rate of  $(3\tau_{\text{irm}})^{-1}$ , one obtains<sup>27</sup>

$$\begin{aligned} \langle \exp(\pm i\phi''(t)) \exp(\mp i\phi''(0)) \rangle \\ = \langle \exp(\pm 2i\phi''(t)) \exp(\mp 2i\phi''(0)) \rangle = \exp(-t/\tau_{\text{irm}}) \end{aligned} \quad (\text{A9})$$

Substituting expressions of the form of eq A7, A8, and A9 into A6 yields

$$\langle F_0(t) F_0(0) \rangle = (A + B + C + D) \sum_{k=1}^s \exp(-t/\tau_{k0}) \quad (\text{A10})$$

$$\begin{aligned} A &= (1/20)(1 - 3 \cos^2 \Delta)^2 + (3/20) \sin^4 \Delta \exp(-t/\tau_{\text{irp}}) \\ &\quad + (3/20) \sin^2 2\Delta \exp(-t/\tau_{\text{irp}}) \\ B &= ((1/8) \sin^4 \Delta + (1/10) \sin^2 \Delta \\ &\quad - (1/40) \sin^2 2\Delta) \exp(-t/\tau_{\text{irm}}) \end{aligned}$$

$$C = (3/40)(1 + \cos^4 \Delta + 6 \cos^2 \Delta) \exp(-t/\tau_{\text{irm}})$$

$$D = (3/10)(\cos^2 \Delta \sin^2 \Delta) \exp(-t/\tau_{\text{irm}})$$

If internal rotation of the methyl group is very rapid ( $\tau_{\text{irm}} \ll \tau_{\text{irp}}$  or  $\tau_{k0}$ ), eq A10 reduces to

$$\langle F_0(t) F_0(0) \rangle = A \sum_{k=1}^s \exp(-t/\tau_{k0}) \quad (\text{A11})$$

This expression differs from the equation based on overall rotatory diffusion, backbone rearrangements, and phenyl group rotation by only a factor of  $(3 \cos^2 \alpha - 1)^2/4$  with  $\alpha = 90^\circ$ . The methyl group rotation reduces the dipolar interactions within the methyl group but makes no contribution to relaxation according to eq A11. The factor  $(3 \cos^2 \alpha - 1)^2/4$  has been given previously to account for the effects of very fast internal rotation.<sup>31</sup> The time averages of the other orientation functions differ from eq A10 and A11 by only multiplicative constants.

$$\begin{aligned} \langle F_1^*(t) F_1(0) \rangle &= (1/6) \langle F_0^*(t) F_0(0) \rangle \\ \langle F_2^*(t) F_2(0) \rangle &= (2/3) \langle F_0^*(t) F_0(0) \rangle \end{aligned} \quad (\text{A12})$$



The spectral densities are obtained by Fourier transformation of either eq A10 or A11, and for eq A11 the results are

$$J_i = 2fK_i \sum_{k=1}^s \frac{A'\tau_{k0}}{1 + \omega_i^2\tau_{k0}^2} + \frac{B'\tau_{bk0}}{1 + \omega_i^2\tau_{bk0}^2} + \frac{C'\tau_{k0}}{1 + \omega_i^2\tau_{k0}^2}$$

$$\tau_{bk0}^{-1} = \tau_0^{-1} + \tau_k^{-1} + \tau_{ir}^{-1} \quad \tau_{k0}^{-1} = \tau_0^{-1} + \tau_k^{-1}$$

$$A' = (3 \cos^2 \Delta - 1)^2/4; B' = (3 \sin^2 2\Delta)/4; C' = (3 \sin^4 \Delta)/4;$$

$$f = (3 \cos^2 \alpha - 1)^2/4 = 1/4; K_0 = 4/5; K_1 = 2/15; K_2 = 8/15.$$

## References and Notes

- (1) A. Allerhand and R. K. Hailstone, *J. Chem. Phys.*, **56**, 3718 (1972).
- (2) J. Schaefer and D. F. S. Natusch, *Macromolecules*, **5**, 416 (1972).
- (3) A. A. Jones, K. Matsuo, K. F. Kuhlmann, F. Geny, and W. H. Stockmayer, *Polym. Prepr., Am. Chem. Soc., Div. Polym. Chem.*, **16**, 578 (1975).
- (4) K. Matsuo, K. F. Kuhlmann, N. W.-H. Yang, W. H. Stockmayer, F. Geny, and A. A. Jones, *J. Polym. Sci., Polym. Phys. Ed.*, **15**, 1347 (1977).
- (5) G. Herman and G. Weil, *Macromolecules*, **8**, 171 (1975).
- (6) W. P. Slichter and D. D. Davis, *Macromolecules*, **1**, 47 (1968).
- (7) Y. Inoue, A. Nishioka, and R. Chujo, *J. Polym. Sci., Polym. Phys. Ed.*, **11**, 2237 (1973).
- (8) F. Heatley, *Polymer*, **16**, 443 (1975).
- (9) J. Spevacek and B. Schneider, *J. Polym. Sci., Polym. Phys. Ed.*, **14**, 1789 (1976).
- (10) A. E. Tonelli, *Macromolecules*, **5**, 558 (1972); **6**, 503 (1973).
- (11) F. Laupretre and L. Monnerie, *Eur. Polym. J.*, **11**, 845 (1975).
- (12) A. A. Jones and W. H. Stockmayer, *J. Polym. Sci., Polym. Phys. Ed.*, **15**, 847 (1977).
- (13) G. C. Staffin and C. C. Price, *J. Am. Chem. Soc.*, **82**, 3632 (1960).
- (14) J. M. Barrales-Rienda and D. C. Pepper, *J. Polym. Sci., Polym. Lett. Ed.*, **4**, 939 (1966).
- (15) A. A. Brooks, J. D. Cutnell, E. O. Stejskal, and V. W. Weiss, *J. Chem. Phys.*, **49**, 1571 (1968).
- (16) I. Solomon, *Phys. Rev.*, **99**, 559 (1955).
- (17) L. G. Werbelow and A. G. Marshall, *J. Magn. Reson.*, **11**, 299 (1973).
- (18) L. G. Werbelow and A. G. Marshall, *J. Am. Chem. Soc.*, **95**, 5132 (1973).
- (19) L. G. Werbelow and D. M. Grant, *J. Chem. Phys.*, **63**, 544 (1975).
- (20) L. G. Werbelow and D. M. Grant, *J. Chem. Phys.*, **63**, 4742 (1975).
- (21) J. Riseman and J. G. Kirkwood, *J. Chem. Phys.*, **16**, 422 (1949).
- (22) A. Isihara, *Adv. Polym. Sci.*, **5**, 531 (1968).
- (23) A. A. Jones and W. H. Stockmayer, *Polym. Prepr., Am. Chem. Soc., Div. Polym. Chem.*, **15**, 16 (1974).
- (24) A. A. Jones, W. H. Stockmayer, and R. J. Molinari, *J. Polym. Sci., Polym. Symp. Ed.*, **54**, 227 (1976).
- (25) B. Valeur, J.-P. Jarry, F. Geny, and L. Monnerie, *J. Polym. Sci., Polym. Phys. Ed.*, **13**, 667 (1975).
- (26) B. Valeur, L. Monnerie, and J.-P. Jarry, *J. Polym. Sci., Polym. Phys. Ed.*, **13**, 675 (1975).
- (27) D. E. Woessner, *J. Chem. Phys.*, **36**, 1 (1962).
- (28) A. A. Jones, *J. Polym. Sci., Polym. Phys. Ed.*, **15**, 863 (1977).
- (29) R. Mattes and E. G. Rochow, *J. Polym. Sci., Part A-2*, **4**, 375 (1966).
- (30) G. Allen, M. W. Coville, R. M. John, and R. F. Warren, *Polymer*, **11**, 490 (1970).
- (31) A. G. Marshall, P. G. Schmidt, and B. D. Sykes, *Biochemistry*, **11**, 3875 (1972).
- (32) J. Schaefer, *Macromolecules*, **6**, 882 (1974).
- (33) R. P. Lubianez and A. A. Jones, *Polym. Prepr., Am. Chem. Soc., Div. Polym. Chem.*, **17**, 138 (1976).
- (34) D. Doddrell, V. Glushko, and A. Allerhand, *J. Chem. Phys.*, **56**, 3683 (1972).
- (35) A. E. Tonelli, *Macromolecules*, **6**, 682 (1973).
- (36) F. Laupretre and L. Monnerie, *Eur. Polym. J.*, **10**, 21 (1974).
- (37) J. Schaefer, E. O. Stejskal, and R. Buchdahl, *Polym. Prepr., Am. Chem. Soc., Div. Polym. Chem.*, **17**, 17 (1976).
- (38) J. Schaefer, E. O. Stejskal, and R. Buchdahl, *Macromolecules*, **10**, 384 (1977).

## Isomobility States in Polymer Liquids

A. A. Miller

1070 Hickory Road, Schenectady, New York 12309. Received July 11, 1977

**ABSTRACT:** A new universal constant,  $-10^4 K = 17 (\pm 1) \text{ cm}^3/(\text{g deg})$ , where  $K = (\partial v/\partial T)_\eta - (\partial v/\partial T)_p$  and  $(\partial v/\partial T)_\eta$  is an isoviscosity volume term, is demonstrated for vinyl-type polymer liquids from Newtonian  $\eta$ - $p$ - $T$  measurements in the literature. For viscosity, this value of  $K$  applies only up to the critical "entanglement" molecular weight,  $M_c$ , but from dielectric relaxation data and  $dT_g/dp$  data at the glass transition the same  $K$  is found for higher molecular weights as well. Results for the  $n$ -alkane series suggest that a main chain of about 15 carbon atoms is the minimum length for a temperature-independent  $K$ . Below this,  $-K$  increases with temperature. A single nonvinyl polymer examined (bisphenol A polycarbonate), containing rigid aromatic groups in the main chain, gives  $-10^4 K = 10 \text{ cm}^3/(\text{g deg})$ . Implications for predicting polymer liquid mobilities at constant temperature and at constant volume are presented. All of the results support the view that the glass transition is an isomobility state which cannot be rigorously defined by thermodynamics alone.

Despite much experimental and theoretical effort over the past two decades the molecular parameters governing mobilities of polymer liquids have yet to be elucidated.

To rigorously test existing theories, or to provide a sound basis for any new ones, requires extensive data on mobilities for a variety of chemical structures over a broad range of  $p$ - $v$ - $T$  conditions down to the glass transition. Toward this end the present work continues the development of new quantitative relationships for Newtonian viscosity, applying also to the more localized motion of the polymer chain as manifested by dielectric relaxation.

Considering Newtonian viscosity as a function of  $p$ ,  $v$ , and  $T$  the following exact relationship was derived by partial differentiation:<sup>1,2</sup>

$$-K = (\partial \ln \eta / \partial T)_p (\partial v / \partial p)_T / (\partial \ln \eta / \partial p)_T \quad (1)$$

where

$$K = (\partial v / \partial T)_\eta - (\partial v / \partial T)_p \quad (2)$$

Since  $(\partial \ln \eta / \partial p)_T / (\partial \ln \eta / \partial T)_p = -(\partial T / \partial p)_\eta$ , substitution in eq 1 gives

$$K = (\partial v / \partial p)_T / (\partial T / \partial p)_\eta \quad (3)$$

For a number of vinyl-type polymers it was found<sup>2</sup> that not only was  $K$  insensitive to temperature but it appeared to be a "universal" constant for these liquids, i.e.,  $-10^4 K = 17 (\pm 1) \text{ cm}^3/(\text{g deg})$ . With  $K$  as a parameter and with polystyrene (PS) as an example, relationships were reported for estimating viscosities at constant volume and at constant temperature.<sup>3</sup> The latter calculations gave pressure coefficients,  $(\partial \ln \eta / \partial p)_T$ , which were independent of pressure up to at least 1000 bars in agreement with experimental observations, indicating that the  $v_\eta$  lines are parallel, as depicted in Figure 1. Preliminary calculations<sup>2</sup> with reported values of  $dT_g/dp$  in eq 3 suggested that the  $v_g$  line, representing the volume at the glass transition for elevated temperatures and pressures, is also parallel to  $v_\eta$ .

At constant (atmospheric) pressure the temperature de-